EFDC+ Tropical Cyclone White Paper

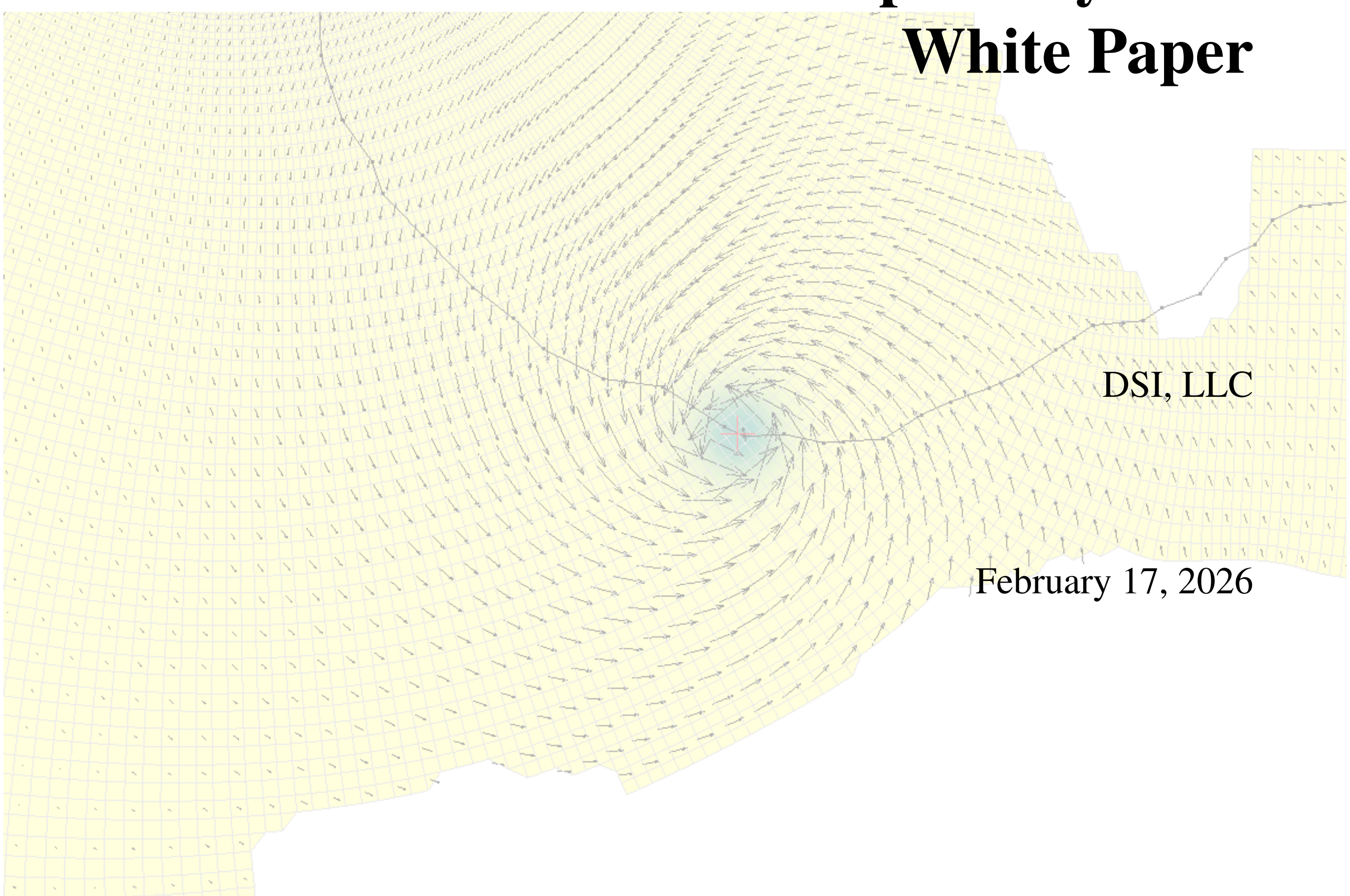

DSI, LLC

February 17, 2026

Edmonds, WA
www.eemodelingsystem.com

This page left intentionally blank.

Contents

List of Tables

List of Figures

List of Abbreviations

ASCII American Standard Code for Information Interchange

EEMS EFDC_Explorer Modeling System

EFDC+ Environmental Fluid Dynamics Code Plus

HURDAT2 Hurricane best track database

JSON JavaScript Object Notation

JTWC Joint Typhoon Warning Center of the U.S Navy

NOAA National Oceanic and Atmospheric Administration of the United States

RSMC Regional Specialized Meteorological Centre

UTC Coordinated Universal Time

UTM Universal Transverse Mercator

1. Introduction

A tropical cyclone is a large system of rapidly rotating winds around a low atmospheric pressure center developing over the tropical waters that produces extreme winds, gusts and heavy rainfall. Depending on its location and strength, it is called a “hurricane” (in the North Atlantic and north-eastern Pacific oceans), “typhoon” (in the northwestern Pacific Ocean), “tropical cyclone” or a “server cyclonic storm” (in the south Pacific and Indian Oceans), “willi-willi” (in the waters near Australia), “tropical storm” or “tropical depression” (at a weaker strength). Due to the Coriolis effect, the rotation of a tropical cyclone is counterclockwise in the Northern Hemisphere whilst it is clockwise in the Southern Hemisphere.

The extreme and rapid changes in atmospheric pressure and wind fields in a tropical cyclone may have strong influences on the hydrodynamics and waves in a water body, especially in the near shore areas. Storm surge induced by pressure depletion and strong winds pile up water against the shore and may cause serious damage as a consequence of coastal inundation and erosion. Beyond the flooding issues due to cyclones, modeling their environmental impacts from erosion, spills, and contaminant transport are essential.

The impacts of a tropical cyclone on a water body are governed by its near surface wind and pressure fields which can be represented using simplified parametric models.

The common approach of a simplified parametric model is to present the fully developed wind fields over the open ocean derived from a steady symmetric vortex that is stationary in a fluid at rest (Harper et al., 2001).

The pressure profile of a tropical cyclone decreases gradually from a relatively flat region outside the cyclone but exponentially towards the minimum value at the cyclone center.

The cyclone wind speed profile increases exponentially towards the center, driven by the increasing pressure gradient and reaches a maximum wind speed at the location of the so-called ”radius of maximum wind speed”, before rapidly dropping to calm in the cyclone center. Figure 1.1 sketches the profiles of sea level pressure and average surface wind speed in a tropical cyclone.

At top of the atmospheric boundary layer, the primary circulation of the cyclone is from the balancing between the pressure gradient force, the Coriolis force and the centrifugal force which resulting the cyclone gradient wind with the wind direction tangent to the isobars. Near the surface, the wind field is converted to the surface winds by consideration of boundary layer effects. This includes wind inflow towards the cyclone center and asymmetric effects due to storm forward motion or surrounding synoptic pressure gradients (Harper et al., 2001).

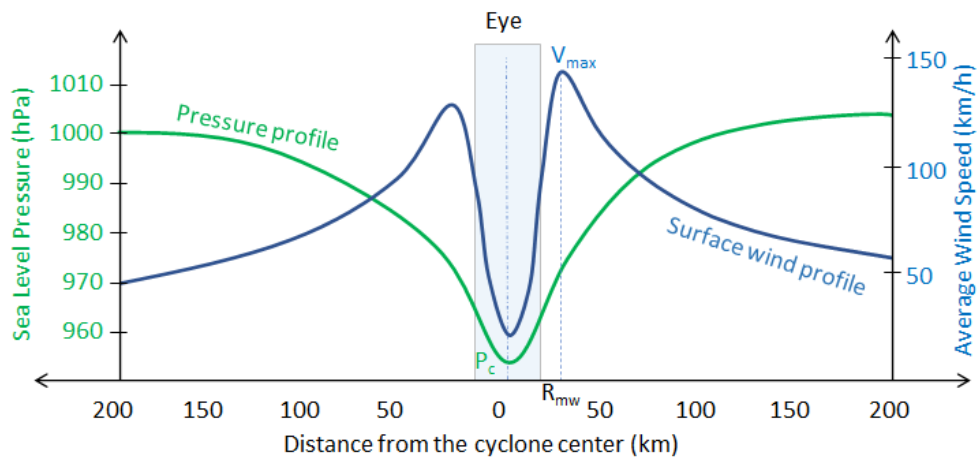

Fig. 1.1. Tropical cyclone pressure and wind profiles.

2. Cyclone parametric models

In EFDC+, four models for tropical cyclones have been implemented including Holland (1980), Hubbert et al. (1991), McConochie et al. (2004) and Willoughby et al. (2006).

2.1. Holland (1980) model

In this model, the atmospheric pressure at a computational point located at a distance r from the cyclone center is

$$P(r) = P_c + (P_n - P_c)\exp\left[-(\frac{R_{mw}}{r})^B\right] \tag{2.1}$$

where,

r	the distance from the computational point to the cyclone center,
P	the atmospheric pressure at the computational point,
P_c	the atmospheric pressure at the cyclone center,
P_n	the ambient pressure,
R_{mw}	the radius of maximum wind speed, and
B	the Holland's shape parameter.

The Holland's shape parameter B has the value ranges from 1 - 2.5 and can be estimated as

$$B = \frac{\rho_a e V_{max}^2}{P_n - P_c} \tag{2.2}$$

where ρ_a is the air density, V_{max} is the sustained maximum wind speed, and e is the exponential growth constant. The transitional speed is subtracted from the observed maximum wind speed from cyclone track data and converted from 10 m above the surface to the top of the boundary layer. This is done to avoid distortion in the Holland curve fit when estimating the B parameter. These will be added back again later.

The wind vector components at the computational point (r, θ) are computed as follows:

$$W_{sx} = V_r \cos\phi + K_f V_{fx} \tag{2.3}$$
$$W_{sy} = V_r \sin\phi + K_f V_{fy} \tag{2.4}$$

where,

- W_{sx} and W_{sy} are the $x-$ and $y-$components of the wind velocity at the computational point, respectively,
- V_{fx} and V_{fy} are the components of the cyclone transitional speed in the $x-$ and $y-$directions, respectively,
- V_r is the 10-minute averaged gradient wind velocity at 10 m above the surface,
- ϕ is the wind angle in the Cartesian coordinate system, $\phi = \pi - \theta$,
- θ is the bearing angle of the computational point measured clockwise from North, and
- K_f is a parameter accounting for the contribution of the cyclone forward speed to the wind velocity. The typical range of this parameter is between 0.5 - 1.0.

The gradient wind velocity at 10 m above the surface V_r is converted from the gradient wind velocity at the top of atmospheric boundary layer V_g:

$$V_r = K_r V_g(r) \tag{2.5}$$

where K_r is the conversion factor with the typical value of $K_r = 0.7$ and V_g is computed as

$$V_g(r) = \sqrt{100B\frac{P_n - P_c}{\rho_a}\left(\frac{R_{mw}}{r}\right)^B \exp\left[-\left(\frac{R_{mw}}{r}\right)^B\right] + \left(\frac{rf}{2}\right)^2} - \frac{|rf|}{2} \tag{2.6}$$

where $f = 2\Omega\sin\varphi$ is the Coriolis parameter, Ω is the angular speed of the Earth, and φ is the latitude.

2.2. Hubbert et al. (1991) model

Hubbert et al. (1991) used Holland (1980) model but applied a constant inflow angle of $\beta = 25°$ and a bearing of the location of the maximum wind speed $\theta_{max} = 70°$ relative to the moving direction θ_f of the cyclone.

The model uses the first order asymmetry factor to add the cyclone translation speed to the wind field

$$K_f = \cos(\theta_f + \theta_{max} - \theta) \tag{2.7}$$

The wind direction is computed from

$$\phi = \pi - \theta + \beta \tag{2.8}$$

Figure 2.1 depicts the direction of surface wind in a tropical cyclone in the Northern Hemisphere.

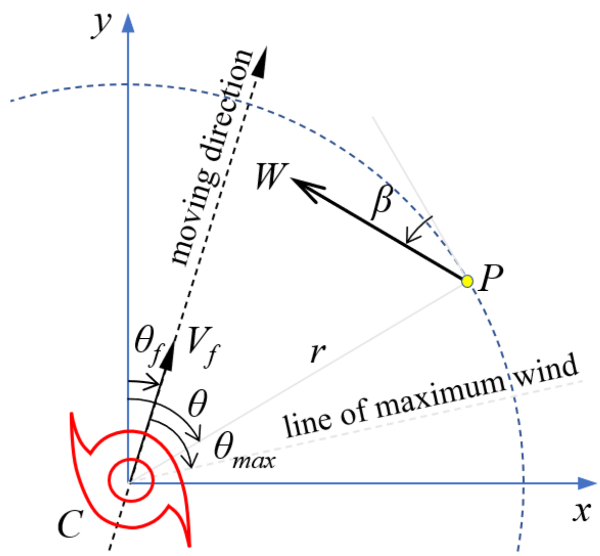

Fig. 2.1. Tropical cyclone wind direction in the Northern Hemisphere.

In this model, if the B parameter is not specified ($B \leq 0$) then it will be calculated as:

$$B = 1.5 + \frac{980 - P_c}{120} \tag{2.9}$$

2.3. McConochie et al. (2004) model

McConochie et al. (2004) model is similar to Hubbert et al. (1991) but uses a distance dependent inflow angle and a wind speed dependent boundary layer coefficient.

$$V_r = f_r V \tag{2.10}$$

where

$$V = V_g + K_f V_f \tag{2.11}$$

The boundary layer coefficient according to Harper et al. (2001) is:

$$f_r = \begin{cases} 0.81, & |V| \leq 6m/s \\ 0.81 - 2.93 \cdot 10^{-3}(|V| - 6), & 6 < |V| \leq 19.5m/s \\ 0.77 - 4.31 \cdot 10^{-3}(|V| - 19.5), & 19.5 < |V| \leq 45m/s \\ 0.66, & |V| \geq 45m/s \end{cases} \tag{2.12}$$

The asymmetry coefficient is determined as

$$K_f = 0.5\left[1+\cos\left(\theta_f+\theta_{max}-\theta\right)\right] \tag{2.13}$$

The inflow angle according to Sobey et al. (1977):

$$\beta = \begin{cases} 10^\circ \frac{r}{R_{mw}}, & 0 \le r < R_{mw} \\ 10^\circ + 75^\circ\left(\frac{r}{R_{mw}}-1\right), & R_{mw} \le r < 1.2R_{mw} \\ 25^\circ, & r \ge 1.2R_{mw} \end{cases} \tag{2.14}$$

2.4. Willoughby et al. (2006) model

The gradient wind speed profile is determined based on the tangential wind component in the eye V_i and the one beyond the transition zone V_o, which lies between $r = R_1$ and $r = R_2$:

$$V_g = \begin{cases} V_i, & r \le R_1 \\ (1-w)V_i + wV_o, & R_1 \le r < R_2 \\ V_o, & r \ge R_2 \end{cases} \tag{2.15}$$

The tangential wind component in the eye V_i

$$V_i = V_{max}\left(\frac{r}{R_{mw}}\right)^n \tag{2.16}$$

The tangential wind component beyond the transition zone V_o,

$$V_o = V_{max}\left[(1-A)\exp\left(\frac{R_{mw}-r}{X_1}\right) + A\exp\left(\frac{R_{mw}-r}{X_2}\right)\right] \tag{2.17}$$

where X_1 is the exponential decay length in the outer vortex:

$$X_1 = 317.1 - 2.026V_{max} + 1.915\varphi \tag{2.18}$$

$X_2 = 25$, n is the exponent for the power law inside the cyclone eye:

$$n = 0.4067 + 0.0144V_{max} - 0.0038\varphi \tag{2.19}$$

A is a parameter to set the proportion of the two exponentials in the wind profile

$$A = 0.0696 + 0.0049V_{max} - 0.0064\varphi \tag{2.20}$$

The weighting function is determined by solving the non-linear equation for the dimensionless unknown ξ

$$\xi = \frac{r-R_1}{R_2-R_1} \tag{2.21}$$

This function ramps up smoothly from zero to one between R_1 and R_2

$$w(\xi) = \begin{cases} 0, & \xi \leq 0 \\ 70\xi^9 - 315\xi^8 + 540\xi^7 - 420\xi^6 + 126\xi^5, & 0 < \xi < 1 \\ 1, & \xi \geq 1 \end{cases} \tag{2.22}$$

with the right hand side

$$w(\xi) = \frac{n\left[(1-A)X_1 + AX_2\right]}{n\left[(1-A)X_1 + AX_2\right] + R_{mw}} \tag{2.23}$$

The gradient wind speed is converted to the surface wind speed using a boundary layer coefficient

$$V_r = f_r V_g \tag{2.24}$$

where the boundary layer coefficient according to Harper et al. (2001) is

$$f_r = \begin{cases} 0.90, & r \leq 100km \\ 0.90 - 0.15\frac{r-100}{600}, & 100 < r < 700km \\ 0.75, & r \geq 700km \end{cases} \tag{2.25}$$

The inflow angle according to Phadke et al. (2003):

$$\beta = \begin{cases} 10^\circ\left(\frac{r}{R_{mw}} + 1\right), & 0 \leq r < R_{mw} \\ 20^\circ + 25^\circ\left(\frac{r}{R_{mw}} - 1\right), & R_{mw} \leq r < 1.2R_{mw} \\ 25^\circ, & r \geq 1.2R_{mw} \end{cases} \tag{2.26}$$

The coefficient accounting for the cyclone asymmetry is calculated as:

$$K_f = \frac{r \cdot R_{mw}}{r^2 + R_{mw}^2} \tag{2.27}$$

If the radius of the maximum wind speed is missing $(R_{mw} \leq 0)$ then it will be computed as

$$R_{mw} = 46.4\exp\left(-0.0155V_{max} + 0.0169\varphi\right) \tag{2.28}$$

3. Data and data processing

3.1. Data files

Environmental Fluid Dynamics Code Plus (EFDC+) simulates tropical cyclones by reading two input files, which contain the module control parameters, and the tropical cyclone tracking data. First, this chapter provides the details of the model parameters and input data necessary for the input files. Then, we suggest general guidelines for cyclone track specifications, which can be used as the model inputs when the required information is missing or unavailable

3.1.1 efdc.inp

"efdc.inp" is the master input file of EFDC+. It is an American Standard Code for Information Interchange (ASCII)-formatted file containing computational options and data setting parameters, structured into card groups with respect to input objectives. In card group 14D, the parameter $ICYCL$ specifies options for whether the tropical cyclone module is activated for a simulation as listed in Table 3.1.

Table 3.1. Tropical cyclone module control fields in efdc.inp file.

Card	Field	Value	Description
C14D	$ICYCL$	0	Do not simulate tropical cyclones
		1	Simulate tropical cyclones using Holland (1980) model
		2	Simulate tropical cyclones using Hubbert et al. (1991) model
		3	Simulate tropical cyclones using McConochie et al. (2004) model
		4	Simulate tropical cyclones using Willoughby et al. (2006) model
	$RHOA$	1.15	The air density, ρ_a in kg/m^3
	$PINF$	1013	The ambient pressure, P_n in hPa
	$THETAM$	65	The bearing angle of maximum wind relative to the forward moving direction of the cyclone, θ_{max} in $degrees$

When $ICYCL = 0$, the tropical cyclone module is not activated. If $ICYCL \geq 0$ and $ICYCL \leq 4$, the tropical cyclone module is activated and the corresponding parametric model of Holland (1980), Hubbert et al. (1991), McConochie et al. (2004), or Willoughby et al. (2006) is used to generate the pressure and wind fields.

3.1.2 cyclones.jnp

“cyclones.jnp” contains all tropical cyclone tracks for EFDC+ simulations in JavaScript Object Notation (JSON) format. Figure 3.1 shows an example of the “cyclones.jnp” file format, and Table 3.2 provides the descriptions for each field grouping with respect to hierarchical levels.


```
{
  "base_date": "2004-01-01",
  "tracks": [
    {
      "basin": "AL",
      "id": "062004",
      "name": "FRANCES",
      "start": 237.0,
      "end": 253.75,
      "points": [
        {
          "time": 237.0,
          "lon": -35.20,
          "lat": 11.10,
          "x": 6067370.60,
          "y": 1735428.56,
          "pc": 1009.0,
          "vmax": 12.8611,
          "rmw": -999.0,
          "vx": -11.063,
          "vy": -1.358,
          "b": 0.0
        },
        {
          "time": 237.25,
          "lon": -36.80,
          "lat": 11.20,
          "x": 5828417.86,
          "y": 1706084.55,
          "pc": 1008.0,
```


Fig. 3.1. An example tropical cyclone track data file.

At the general level, “base_date” is reference data for all timing values of the track points in the file. This reference data is normally set the same as the EFDC+ model’s base date. All tropical cyclone tracks are stored in the "tracks" array. Each tropical cyclone track starts with a header of metadata fields such as storm basin, tropical cyclone ID and name, and start and end time of the current track with respect to the "base_date". All of these fields are only for reference only and not used by EFDC+ during the simulation. The actual track point data used in the simulation are stored in the "points" array of each tropical cyclone track.

Table 3.2. Tropical cyclone track point data fields in cyclones.jnp file.

Field	Units	Description
time	*days*	Julian days since the "base_date"
lon	*degrees*	Longitude of the tropical cyclone center in *degrees*
lat	*degrees*	Latitude of the tropical cyclone center in *degrees*
x	*m*	UTM x-coordinate of the tropical cyclone center in *meters*
y	*m*	UTM y-coordinate of the tropical cyclone center in *meters*
pc	*hPa*	Minimum central pressure at cyclone center, P_c in *hPa* or *mb*
vmax	m/s	Maximum wind speed, V_{max} in m/s
rmw	*km*	Radius maximum wind, R_{mw} in *km*
vx	m/s	X-component of the tropical cyclone translation speed, V_{fx} in m/s
vy	m/s	Y-component of the tropical cyclone translation speed, V_{fy} in m/s
b	-	Holland's B parameter

3.2. Data sources

Tropical cyclone tracks are available online at different web sites for different storm basins over the world. The basic track data normally including the time (in Coordinated Universal Time (UTC)), eye location (longitude and latitude), central pressure and sometimes the maximum wind speed and the radius of maximum wind.

Some of the cyclone track formats supported by EFDC_Explorer Modeling System (EEMS) are:

– **National Oceanic and Atmospheric Administration of the United States (NOAA)** Cyclone tracks are provided in Hurricane best track database (HURDAT2) format with two datasets: the Atlantic hurricane database for 1851-2020 and the Northeast and North Central Pacific hurricane database for 1949-2020.

– **Joint Typhoon Warning Center of the U.S Navy (JTWC)** The JTWC best track data source includes the following datasets: Southern Hemisphere (1945-2019), Northern Indian Ocean (1945-2019), and Western North Pacific Ocean (1945-2019).

– **RSMC (Regional Specialized Meteorological Centre)** There are six regional centers which provide cyclone track forecasts and archives for different regions around the world as shown in Table 3.3.

Table 3.3. Tropical Cyclone Regional Specialised Meteorological Centres (RSMCs) in the world.

RSMC Miami-Hurricane Center NOAA/NWS National Hurricane Center, USA.	The Caribbean Sea, Gulf of Mexico, North Atlantic and eastern North Pacific Oceans
RSMC Tokyo-Typhoon Centre Japan Meteorological Agency.	Western North Pacific Ocean, and the South China Sea
RSMC-tropical cyclones New Delhi India Meteorological Department.	North Indian Ocean The Bay of Bengal and the Arabian Sea
RSMC La Réunion-Tropical Cyclone Centre Météo-France.	South-West Indian Ocean (including the Mozambique Channel)
RSMC Nadi-Tropical Cyclone Centre Fiji Meteorological Service.	South-West Pacific Ocean,
RSMC Honolulu-Hurricane Center NOAA/NWS, USA.	Central North Pacific Ocean

3.3. Data processing

EEMS has utilities to process tropical cyclone track data to fill in all track data fields that required for EFDC+ simulations. This includes the conversion of cyclone eye location from longitude and latitude to Universal Transverse Mercator (UTM) coordinates, computing the translation speed and heading and filling the missing data.

3.3.1 Translation speed

Firstly, the geographic locations of the tropical cyclone centers at different times are converted into UTM coordinates using the EFDC+ model UTM zone. Then the translation speed of the is computed

$$V_{fx} = \frac{x_{i+1} - x_i}{t_{i+1} - t_i} \tag{3.1}$$

$$V_{fy} = \frac{y_{i+1} - y_i}{t_{i+1} - t_i} \tag{3.2}$$

where,

V_{fx} and V_{fy} are the components of the cyclone translation speed in the $x-$ and $y-$directions in m/s, respectively,

t_i and t_{i+1} are the times of the data points i and $i+1$ in *seconds*, respectively,

x_i and x_{i+1} are the UTM x-coordinates of the data points i and $i+1$ in *meters*, respectively,

y_i and y_{i+1} are the UTM y-coordinates of the data points i and $i+1$ in *meters*, respectively,

The magnitude of the cyclone translation speed V_{fm} and its bearing angle θ_f are computed as

$$V_{fm} = \sqrt{V_{xy}^2 + V_{fy}^2} \tag{3.3}$$

$$\theta_f = \frac{\pi}{2} - arctan\frac{V_{fy}}{V_{fx}} \tag{3.4}$$

3.3.2 Central pressure

The missing central pressure P_c can be filled with different formulae based on the availability of the maximum wind speed, the radius of maximum wind and others as follows.

Graham and Nunn (1959)

$$P_c = P_n - \left(\frac{V_{max} + f \cdot R_{mw}}{5.61}\right)^2 \tag{3.5}$$

when both V_{max} and R_{mw} are available or

$$P_c = P_n - 33.86 \cdot \ln \frac{R_{mw} - 28.25\tanh\left(0.0873\left(\varphi - 28\right)\right) - 0.2V_{fm} - 37.2}{12.22} \tag{3.6}$$

when only R_{mw} is available.

Kraft (1961)

$$P_c = P_n - \left(\frac{V_{max}}{7.20}\right)^2 \tag{3.7}$$

Fujita (1971)

$$P_c = P_n - \left(\frac{V_{max}}{4.89}\right)^{1.733} \tag{3.8}$$

Atkinson and Holiday (1977)

$$P_c = P_n - \left(\frac{V_{max}}{3.45}\right)^{1.553} \tag{3.9}$$

Holland (1980)

$$P_c = P_n - \frac{\rho_a V_{max}^2}{100eB} \tag{3.10}$$

Dvorak (1984)

$$P_c = P_n - \left(\frac{V_{max}}{3.4}\right)^{1.543} \tag{3.11}$$

Banton et al. (2002)

$$P_c = 748 + 58.82 \cdot \ln R_{mw} \tag{3.12}$$

Kawai et al. (2005)

$$P_c = 687 + 61.5 \cdot \ln R_{mw} \tag{3.13}$$

Takagi et al. (2012)

$$P_c = 846 + 1.3 \cdot R_{mw} \tag{3.14}$$

Lam (2018)

$$P_c = P_n - 0.1747 \cdot V_{max}^{1.5566} \tag{3.15}$$

3.3.3 Maximum wind speed

For the missing maximum wind speed V_{max}, it can be filled with several formulae available from EEMS user interface that including

Graham and Nunn (1959)

$$V_{max} = 5.61\,(P_n - P_c)^{0.5} - f \cdot R_{mw} \tag{3.16}$$

Kraft (1961)

$$V_{max} = 7.20\,(P_n - P_c)^{0.5} \tag{3.17}$$

Fujita (1971)

$$V_{max} = 4.89\,(P_n - P_c)^{0.577} \tag{3.18}$$

Atkinson and Holiday (1977)

$$V_{max} = 3.45\,(P_n - P_c)^{0.644} \tag{3.19}$$

Holland (1980)

$$V_{max} = \sqrt{100B\frac{P_n - P_c}{\rho_a}e} \tag{3.20}$$

Dvorak (1984)

$$V_{max} = 3.4\,(P_n - P_c)^{0.648} \tag{3.21}$$

3.3.4 Radius of maximum wind

For the missing radius of maximum wind R_{mw}, the following formulae can use to fill from EEMS user interface

Graham and Nunn (1959)

$$R_{mw} = 28.25 \tanh\left[0.0873\left(\varphi - 28\right)\right] + 12.22 \exp\left(\frac{P_n - P_c}{33.86}\right) + 0.2 \cdot V_{fm} + 37.2 \tag{3.22}$$

Banton et al. (2002)

$$R_{mw} = 3.0 \times 10^{-6} \exp\left(0.017 \cdot P_c\right) \tag{3.23}$$

Kawai et al. (2005)

$$R_{mw} = 94.89 \exp\left(\frac{P_c - 967}{61.5}\right) \tag{3.24}$$

Willoughby and Rahn (2004)

$$R_{mw} = 46.29 \exp\left(-0.0153 V_{max} + 0.0166\varphi\right) \tag{3.25}$$

Willoughby et al. (2006)

$$R_{mw} = 46.4 \exp\left(-0.0155 V_{max} + 0.0169\varphi\right) \tag{3.26}$$

Knaff and Zehr (2002)

$$R_{mw} = 66.785 - 0.09102 V_{srm} + 1.0619\left(\varphi - 25\right) \tag{3.27}$$

where φ is the latitude of the cyclone center and

$$V_{srm} = V_{max} - 1.5 V_{fm}^{0.63} \tag{3.28}$$

Takagi et al. (2012)

$$R_{mw} = 80 - 0.769\left(950 - P_c\right) \tag{3.29}$$

3.3.5 Holland's B parameter

For the Holland's B parameter, it can be filled with a constant or one of the following formulae

Holland (1980)

$$B = \frac{\rho_a e V_{max}^2}{P_n - P_c} \tag{3.30}$$

or an empirical formula

$$B = 2 - \frac{P_c - 900}{160} \tag{3.31}$$

Young (1999)

$$B = 1.5 - \frac{980 - P_c}{120} \tag{3.32}$$

Willoughby and Rahn (2004)

$$B = 0.886 + 0.0177V_{max} - 0.0094\varphi \tag{3.33}$$

4. Model verification

The cyclone wind models were verified with the Hurricane Katrina in 2005 for several locations with observations along the Gulf Coast. Observed wind speed during the Hurricane Katrina can be downloaded from tidesandcurrents.noaa.gov. The locations for model verification are showed in 4.1 and listed in Table 4.1.

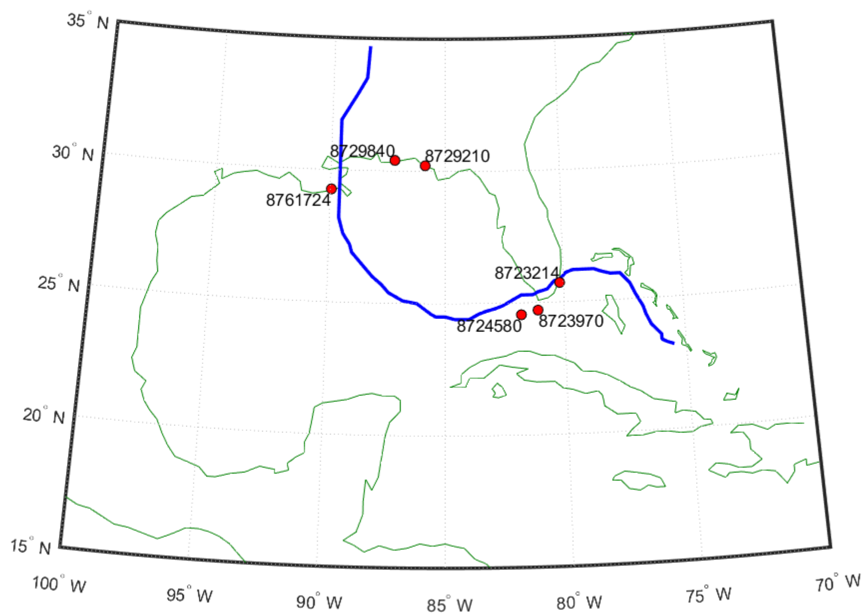

Fig. 4.1. Locations of wind observations (red dots) and track of Hurricane Katrina in 2005 (blue line).

Figures 4.2 to 4.7 showing the comparisons of wind speed computed using different tropical cyclone models with the observed data at the locations.

Table 4.1. Locations of wind data available for model verification.

ID	Name	State	Longitude	Latitude
8723214	Virginia Key, Biscayne Bay	FL	-80.161667	25.731667
8723970	Vaca Key, Florida Bay	FL	-81.106500	24.711000
8724580	Key West	FL	-81.808060	24.550830
8729210	Panama City Beach	FL	-85.878304	30.213301
8729840	Pensacola	FL	-87.211194	30.404389
8761724	Grand Isle	LA	-89.957000	29.263000

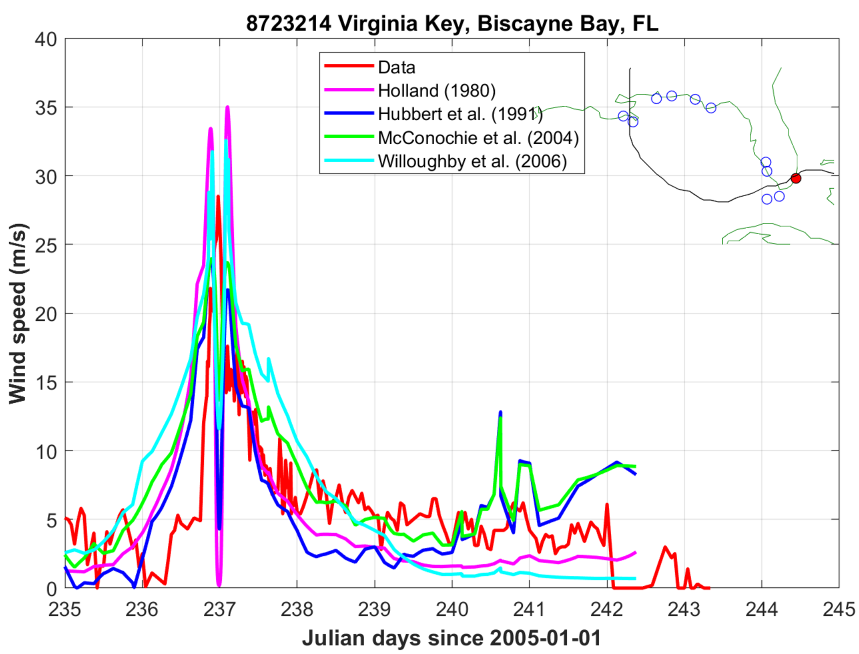

Fig. 4.2. Comparison of wind speed at Virginia Key, Biscayne Bay, FL.

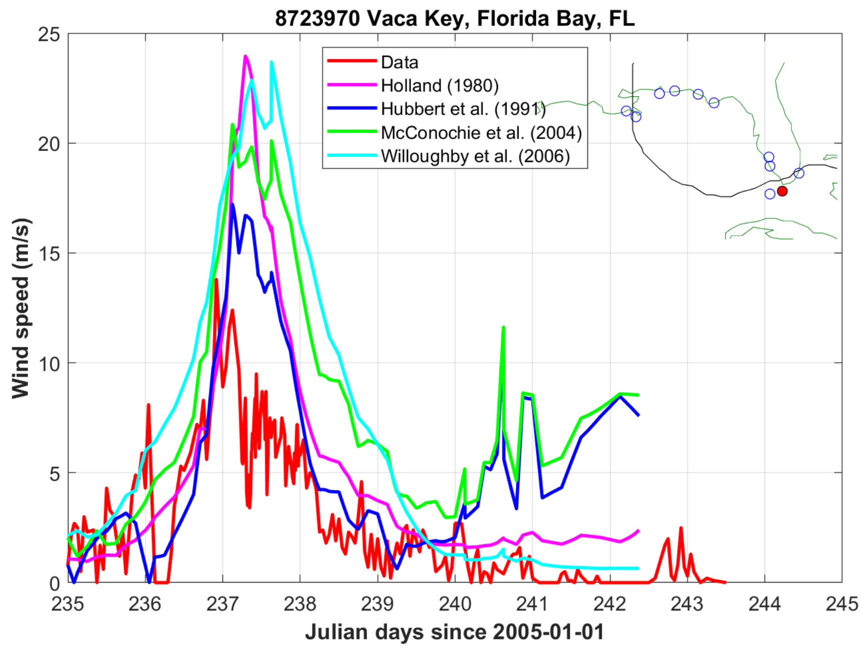

Fig. 4.3. Comparison of wind speed at Vaca Key, Florida Bay, FL.

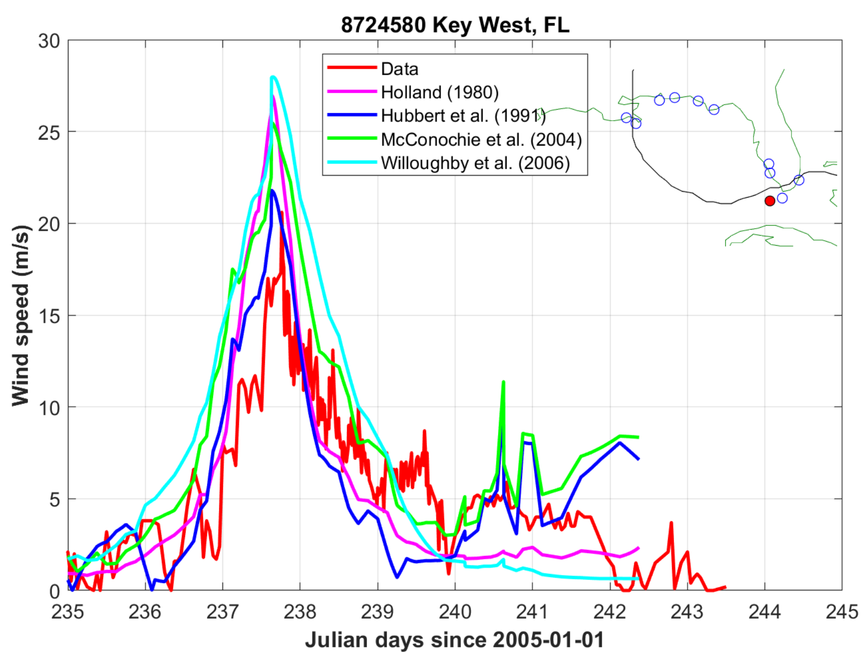

Fig. 4.4. Comparison of wind speed at Key West, FL.

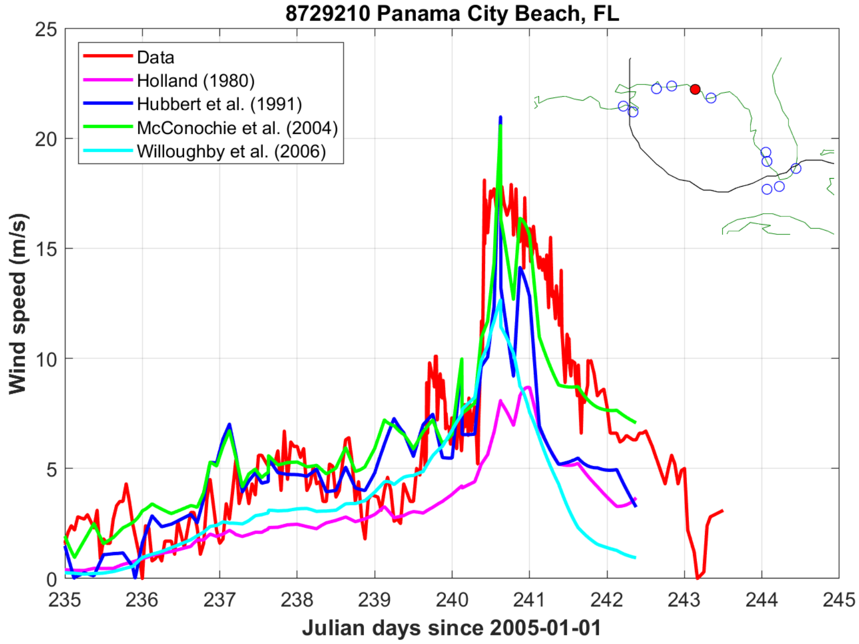

Fig. 4.5. Comparison of wind speed at Panama City Beach, FL.

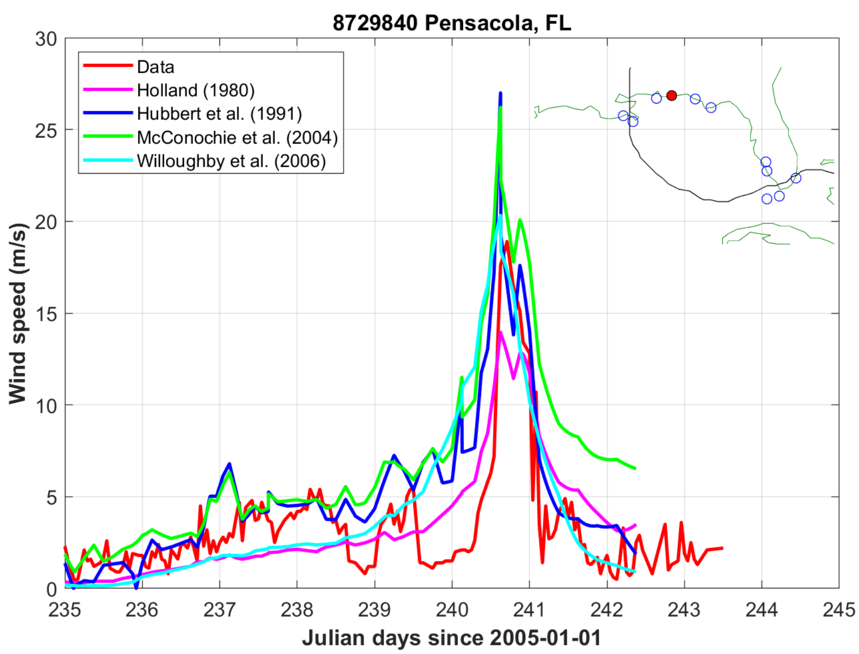

Fig. 4.6. Comparison of wind speed at Pensacola, FL.

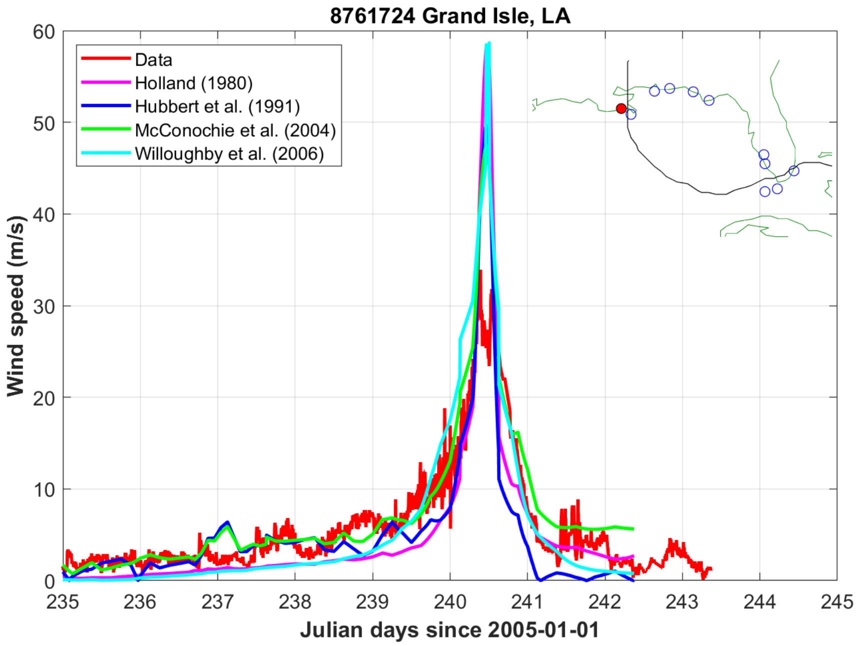

Fig. 4.7. Comparison of wind speed at Grand Isle, AL.

References

G. D. Atkinson and C. R. Holiday. Tropical cyclone minimum sea level pressure/maximum sustained wind relationship for the western north pacific, 1977.

J.D. Banton, D.A.Y. Smith, and P.S. Warner. Long term variability of hurricane trends and a monte carlo approach to design, 2002.

V. Dvorak. Tropical cyclone intensity analysis using satellite data. noaa tech. rep. nesdis 11, 1984.

T. Fujita. Proposed characterization of tornadoes and hurricanes by area and intensity, 1971.

H.E. Graham and D.E. Nunn. Meteorological considerations pertinent to standard project hurricane, atlantic and gulf coasts of the united states, 1959.

B. Harper, T. Hardy, and L. Mason. Queensland climate change and community vulnerability to tropical cyclones: Ocean hazards assessment stage 1, 2001.

G. J. Holland. An analytic model of the wind and pressure profiles in hurricanes, 1980.

G.D. Hubbert, G.J. Holland, L.M. Leslie, and M.J. Manton. A real-time system for forecasting tropical cyclone storm surges, 1991.

H. Kawai, K. Honda, T. Tomita, and T. Kakinuma. Characteristic of typhoons in 2004 and forecasting and hindcasting of their storm surges, 2005.

J.A. Knaff and R.M. Zehr. Reexamination of tropical cyclone wind–pressure relationships, 2002.

R. H. Kraft. The hurricane's central pressure and highest wind, 1961.

N.T. Lam. Influences of manmade structures on storm surge flooding, 2018. ISSN 978.604.82.2483.7.

J.D. McConochie, T.A. Hardy, and L.B. Mason. Modelling tropical cyclone over-water wind and pressure fields, 2004.

A. C. Phadke, C. D. Martino, K. F. Cheung, and S. H. Houston. Modeling of tropical cyclone winds and waves for emergency management, 2003.

R.J. Sobey, B.A. Harper, and K.P. Stark. Numerical simulation of tropical cyclone storm surge, 1977.

H. Takagi, D. Nguyen, M. Esteban, T. Tran, H.L. Knaepen, and T. Mikami. Vulnerability of coastal areas in southern vietnam against tropical cyclones and storm surges, 2012.

H. E. Willoughby and M. E. Rahn. Parametric representation of the primary hurricane vortex. part i: Observations and evaluation of the holland (1980) model, 2004.

H. E. Willoughby, R. W. R. Darling, and M. E. Rahn. Parametric representation of the primary hurricane vortex. part ii: A new family of sectionally continuous profiles, 2006.

I.R. Young. Wind generated ocean waves, 1999.